



# Observed changes in stratospheric circulation: Decreasing lifetime of N<sub>2</sub>O, 2005-2021

Michael J. Prather<sup>1</sup>, Lucien Froidevaux<sup>2</sup>, Nathaniel J. Livesey<sup>2</sup>

<sup>1</sup>Earth System Science Department, University of California Irvine; Irvine, CA 92697-3100, USA

<sup>2</sup>Jet Propulsion Laboratory, California Institute of Technology; Pasadena, CA 91011, USA

Correspondence to: Michael Prather (mprather@uci.edu)

**Abstract.** Using Aura Microwave Limb Sounder satellite observations of stratospheric nitrous oxide (N<sub>2</sub>O), ozone, and temperature from 2005 through 2021, we calculate the atmospheric lifetime of N<sub>2</sub>O to be decreasing. Because N<sub>2</sub>O abundances in the middle tropical stratosphere, where it is photochemically destroyed, increased at a faster rate than the bulk N<sub>2</sub>O in the lower atmosphere, the lifetime is becoming shorter. The cause appears to be a more vigorous stratospheric circulation, which models predict to result from climate change. If this climate-driven circulation trend continues to 2100, then anthropogenic N<sub>2</sub>O emissions will be removed 20% faster than current projections, and their impact on global warming and ozone depletion will be proportionately lessened. This finding is an example of a distinct negative, but relatively minor, climate-chemistry feedback.

## 1 Introduction

Projections of climate change include the acceleration of the stratospheric overturning circulation over the 21<sup>st</sup> century (Abalos et al., 2021). This three-dimensional circulation, condensed into a two-dimensional framework called the Brewer-Dobson Circulation (BDC), brings tropospheric air into the tropical stratosphere where it ascends, being photochemically processed with ultraviolet radiation that increases with altitude, mixes across latitudes, and then descends at mid- to high-latitudes, re-entering the troposphere around mid-latitudes (Plumb and Mahlman, 1987; Neu and Plumb, 1999; Butchart, 2014). Observational metrics for an enhanced BDC are based on trends in the Age-of-Air (AoA) using gases such as SF<sub>6</sub>, but these observations run counter to the climate model projections (Karpechko et al., 2018; Abalos et al., 2021; Garney et al., 2022), in part because the comparison of models and measurements has proven difficult (Fritsch et al., 2020). The search for BDC change with AoA has



missed a more obvious and compelling case based on the important greenhouse gas nitrous oxide  
30 ( $\text{N}_2\text{O}$ ), where recent work has shown agreement in upper stratospheric trends across satellite  
instruments and a model (Froidevaux et al., 2022). Here we take the Aura MLS observations of  $\text{N}_2\text{O}$ ,  
ozone ( $\text{O}_3$ ), and temperature (T) from 2005 through 2021 and show that  $\text{N}_2\text{O}$  increases through the  
middle tropical stratosphere lead to a shorter lifetime, an important consequence of a more vigorous  
BDC.

35

Consequences of an enhanced BDC often focus on the increased flux of stratospheric ozone ( $\text{O}_3$ ) into  
the troposphere with subsequent increase in tropospheric  $\text{O}_3$ , see discussion in (Karpechko et al., 2018;  
Garney et al., 2022). Enhanced BDC also leads to shorter lifetimes for gases like nitrous oxide ( $\text{N}_2\text{O}$ )  
and chlorofluorocarbons (CFCs) as greater abundances are pushed higher in the tropical stratosphere  
40 where they experience greater photolytic destruction. Using the simultaneous MLS vertical profiles of  
 $\text{N}_2\text{O}$ ,  $\text{O}_3$ , and temperature, we calculate the total loss of  $\text{N}_2\text{O}$  in the column, needing only the solar  
spectrum and absorption cross sections, as in Prather et al. (2015). We find that the stratospheric  $\text{N}_2\text{O}$   
loss rate is increasing faster than the observed trend in surface  $\text{N}_2\text{O}$ , and hence the  $\text{N}_2\text{O}$  lifetime is  
declining. For  $\text{N}_2\text{O}$ , a major greenhouse gas, it means that the climate impact of its anthropogenic  
45 emissions will be reduced over this century; and for CFCs where we expect parallel results, it means  
that these now-banned ozone-depleting gases will be cleaned out of the atmosphere faster.

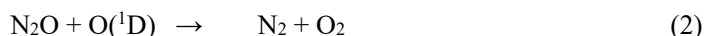
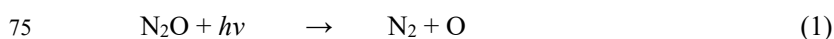
## 2 Measurements and methods

50 The Aura MLS observations of  $\text{N}_2\text{O}$ ,  $\text{O}_3$ , and temperature (T) are taken from the Goddard Earth  
Sciences Data and Information Services Center in the form of Version 5 Level 3 monthly binned  
profiles from August 2004 through December 2021 (Lambert et al., 2021; Schwartz et al., 2021a,  
2021b). All data are averaged over the 72 longitude bins. The very few negative  $\text{O}_3$  values (0.04% of  
data at 0.01 hPa) occur at the minimum in the  $\text{O}_3$  profile and are replaced with the mean value of 0.2  
55 ppm, with negligible impact on photolysis rates. The negative  $\text{N}_2\text{O}$  values are slightly more frequent  
(about 0.1% of data at 32 and 22 hPa, but 1.6% at 0.5 hPa where the mean value is 2.3 ppb). We do not



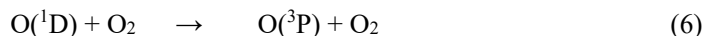
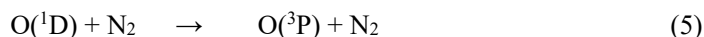
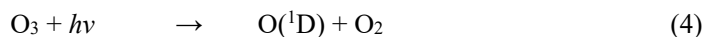
wish to inflate the N<sub>2</sub>O loss by replacing negative values with large positive ones, so we opt for the safest choice and just replace negative N<sub>2</sub>O values with 1 ppb, again, with negligible impact on N<sub>2</sub>O loss. The N<sub>2</sub>O vertical grid between 146 and 1 hPa (6 evenly space log(pressure) levels per decade) is  
 60 coarser than that of O<sub>3</sub> and T (both use the same 12 intervals per decade). The missing N<sub>2</sub>O levels in the O<sub>3</sub>-T grid are calculated as the square-root of the values on the adjacent levels. For pressures <0.4 hPa, where MLS V5 N<sub>2</sub>O data are lacking, we set the abundance to 0 ppb. Polar areas outside the observations (86°-90°) are included in the weighting of the 86° profile. The dataset then covers: 43  
 latitudes (84°S to 84°N), 37 pressure levels (100 – 0.001 hPa), and 209 months (Aug 2004 to Dec  
 65 2021).

The observational data consists of 8,987 independent column atmospheres. The top level (0.001 hPa) is high enough that only a single layer of thickness 0.001 hPa with the same properties as the top layer is added to complete the atmosphere for the radiative calculation. Below 100 hPa, we add 6 layers with  
 70 typical tropospheric composition, but these layers do not much affect the stratospheric N<sub>2</sub>O loss because very little of the critical radiation in these ultraviolet wavelengths reaches the troposphere. For each column we calculate the profile of N<sub>2</sub>O loss from photolysis (J-N<sub>2</sub>O) and reaction with the atomic oxygen radical O(<sup>1</sup>D) from the three reactions:



The O(<sup>1</sup>D) is calculated from the O<sub>3</sub>-T profiles assuming production equals loss

80





85 The radiative transfer calculation is the same as in Prather et al. (2015) and includes the solar  
declination for the middle of each month, the sun-earth distance, but not the solar cycle (a mean solar  
flux is used). During the MLS Aura record used here, we believe that the solar cycle has had little  
impact: the period 2005-2011 following Cycle 23 showed low activity (smoothed monthly sunspot  
number  $< 50$ ); the peak of Cycle 24 (2011-2015) was among the lowest in the last 100 years; and Cycle  
90 25 began in 2020 but activity remained low through 2021. We conclude that the impact of the solar  
cycle on these observations was much less than the min-to-max decrease in  $\text{N}_2\text{O}$  lifetime of 4-7 % (see  
P2015) and probably less than 2-3%. Moreover, the symmetry of this low solar activity over 2005-2021  
is unlikely to affect trends.

95 Vertically, losses are weighted linearly in pressure (mass); and across latitude, they are weighted by the  
area of each latitude belt. Annually integrated budgets include the number of days in each month, but  
leap-years are treated as 365-day years, and thus our annual losses are biased low by 0.07%. Lifetimes  
are budgetary time scales and calculated as a 12-month burden ( $\text{TgN}$ ) divided by the 12-month loss  
( $\text{TgN/yr}$ ). The burden is calculated from monthly-mean, globally-averaged NOAA marine surface  
100 measurements (Dlugokencky, 2022) and using the conversion factor of 4.78  $\text{TgN/ppb}$  (Prather et al.,  
2012). Given that the gridding and source files have changed since P2015, we compared the global  
monthly loss rates for the overlap period with P2015 (Aug 2004 – Dec 2011): the mean difference of  
0.2% and rms difference of 0.6% show that both calculations are essentially identical.

105 Uncertainties in trends here are calculated from a linear regression of the 12-month running averages of  
the monthly means as reported or calculated here. We select the 68% (1-sigma) range, because we are  
looking for 'likely' connections (68% confidence) rather than 'extremely likely' (95%). For example, the  
linear regression trend in  $\text{N}_2\text{O}$  loss uses the running averages and has 198 monthly points. The  
uncertainty is scaled up assuming there are only 17 yearly data points. As a check we recalculate the  
110 regression fit with the unsmoothed monthly data and get the same uncertainty.

### 3 Results



The primary calculation here is the annual  $\text{N}_2\text{O}$  loss ( $\text{TgN/yr}$ ) shown in Figure 1a. It was surprising in  
115 that a clear 17-year increase is apparent. Most of the interannual variability in this 12-month running  
mean time series is associated with the quasi-biennial oscillation (see Ruiz et al., 2021). The linear  
regression gives a trend of  $+5.0 \pm 0.7$  %/decade. This is larger than the  $+2.9 \pm 0.02$  %/decade trend in the  
burden (Figure 1b), and results in an  $\text{N}_2\text{O}$  budgetary lifetime trend of  $-2.1 \pm 0.7$  %/decade (Figure 1c).  
Our best estimate for the  $\text{N}_2\text{O}$  lifetime over the past decade (117 yr) is still close to that in P2015, which  
120 included other model calculations. Most important for the  $\text{N}_2\text{O}$  budget is the average loss itself, namely  
 $13.43 \text{ TgN/yr}$  with an interannual standard deviation of 3% and min-to-max range of 7%. The primary  
source of stratospheric odd-nitrogen species (e.g.,  $\text{NO}$ ,  $\text{NO}_2$ ,  $\text{HNO}_3$ ) is production of  $\text{NO}$  in reaction (3),  
and we calculate the production of  $\text{NO}$  (Figure 1d), which (like the  $\text{N}_2\text{O}$  loss) also shows a positive  
trend of  $+3.9 \pm 0.6$  %/decade.

125

The cause of the lifetime trends can be a change in the photochemical loss frequency, or an increase in  
the abundance of  $\text{N}_2\text{O}$ . The critical zone for loss in the vertical is 3 to 30 hPa (80% of total loss) and in  
latitude it is  $30^\circ\text{S}$  to  $30^\circ\text{N}$  (75%), see P2015, and thus we focus on the tropical middle stratosphere.  
Photolysis (reaction 1) dominates loss here (by more than 90%) and the monthly mean  $\text{J-N}_2\text{O}$  at the  
130 equator (Figure 1e) shows only a consistent decline across the critical region from  $-0.5 \pm 0.1$  %/decade at  
the top of the region (3 hPa) to  $-1.3 \pm 0.3$  %/decade at altitudes below 10 hPa. This decline would reduce  
the loss.

The declining  $\text{J-N}_2\text{O}$  is clearly due to the recovery of overhead ozone during this period from reduced  
135 chlorine-catalyzed depletion as the CFCs and other chlorinated gases have declined following the  
Montreal Protocol agreement that regulated these source gases (Bernath et al., 2020; Froidevaux et al.,  
2022; and references therein). Observations show continued increases in upper tropical stratospheric  
ozone for 2000–2020 (Godin-Beekmann et al., 2022) from a range of satellite measurements, including  
the MLS  $\text{O}_3$  used here that is driving the change of  $\text{J-N}_2\text{O}$ . For the upper stratospheric tropics (1–10  
140 hPa), the generally observed  $\text{O}_3$  trend of order  $+1.0$  to  $+1.6$  %/decade is consistent with the vertical



pattern and magnitude of the J-N<sub>2</sub>O trend. This trend reduces the N<sub>2</sub>O loss and makes disagreement between the burden and loss trends greater.

Given that N<sub>2</sub>O loss is increasing faster than the global burden by +2.1 %/decade, we expect that the  
145 N<sub>2</sub>O abundances in the critical zone are likewise increasing faster. Because of the reduction in  
photolysis rates, we expect the abundance to be increasing at about +6 %/decade. Can we see this in the  
MLS N<sub>2</sub>O data? The monthly mean 30°S-30°N N<sub>2</sub>O abundances are shown in Figure 1f. The trends  
are clear but vary over altitude. At the bottom of the critical zone (32 hPa) the trend is negative, -  
3.4±0.5 %/decade and probably due to a residual negative drift of the V5 MLS data in the lower  
150 stratosphere after 2010 as shown in Figure 16 of Livesey et al. (2021). It is unlikely to be real because  
suppression of N<sub>2</sub>O below 30 hPa can hardly lead to increases above, and moreover the ACE-FTS data  
show positive trends at these pressures following the analysis of Froidevaux et al. (2022). The trend  
increases rapidly reaching +5.5±1.2 %/decade in the central zone (10 hPa) and +12.0±2.3 %/decade  
near the top (4.6 hPa). These increases are used directly in our calculation and average to +6 %/decade  
155 needed to explain the trend in total N<sub>2</sub>O loss.

Are these increases in N<sub>2</sub>O real or an artefact of a known calibration drift in the MLS 190 GHz (mainly  
water vapor and N<sub>2</sub>O) observations? The MLS Version 5 dataset benefits from an extensive effort to  
remove/reduce drifts and verify the MLS H<sub>2</sub>O and N<sub>2</sub>O against the overlapping ACE-FTS satellite  
160 measurements, which are not believed to be drifting (Livesey et al., 2021; Froidevaux et al., 2022). The  
key comparison is Figure 16 of Livesey et al. (2021). In the tropics (20°S-20°N) there could be a small  
positive drift in MLS V5 N<sub>2</sub>O versus ACE-FTS N<sub>2</sub>O for the period 2005-2010 in the range 3-30 hPa,  
but for the later period 2010-2019, there is no drift, or even a negative drift at 30 hPa and below. This  
change with altitude may explain the small or negative trend in N<sub>2</sub>O below 15 hPa. It is possible that  
165 N<sub>2</sub>O is increasing throughout the tropical stratosphere if the negative trend at 32 hPa is due to  
instrumental drift. Parallel analysis of the MLS V4 N<sub>2</sub>O (not shown) shows a similar increase in the  
trend from small negative trends at 32 hPa to large positive ones at 3 hPa (not shown). At the upper end  
of our range (2.2-6.8 hPa), Froidevaux et al. (2022, their Figure 12) find similar trends in N<sub>2</sub>O to ours



(~13 %/decade) from MLS, ACE-FTS, and a model. Their analysis included a much wider latitude  
170 range (50°S-50°N), but because N<sub>2</sub>O abundances fall off rapidly outside of the tropical ascent region  
(see Figure 3 of Prather et al., 2015), the tropics should dominate the mean value and its trend.

#### 4 Implications

175 The recent WMO Ozone Assessments (Karpechko et al., 2018; Garny et al., 2022) concluded that  
disagreement remains regarding the direction of the BDC trend between the chemistry-climate model  
simulations (increasing rates) and the satellite observations (decreasing or uncertain). We present clear  
observational evidence supporting the models of what is likely a climate-change driven increase in the  
net BDC using a major trace gas. N<sub>2</sub>O abundances in the tropical upper stratosphere are increasing at  
180 rates much faster than tropospheric abundances, but this pattern cannot distinguish between more rapid  
ascent or reduced mixing with extra-tropical latitudes. The latter would imply a slower growth rate for  
extra-tropical N<sub>2</sub>O, but this is not seen. If we perform a similar trend analysis to that shown in Figure 1f  
for the extra-tropics (i.e., 30°N-58°N and 30°S-58°S), then we find an almost identical pattern to that in  
the tropics: increasing at 7-8 %/decade versus 6 at 10 hPa; and at 14-18 %/decade versus 13 at 3.2 hPa,  
185 see Supplement Figure S1ab and Table S6. The obvious explanation is an increase in the meridional  
mean ascent rate in the tropics with little or no change in mixing across the barrier between tropics and  
extra-tropics. The use of an integrated quantity like the N<sub>2</sub>O lifetime provides robust averaging over the  
large seasonal and interannual variability of this gas in the middle and upper stratosphere. We expect  
these results to hold for other gases with mid-stratosphere photolytic sinks, such as CFC-12.

190  
Viewing the changing BDC in terms of lifetimes gives a different perspective of the potential  
consequences of climate change. If this rate of change continues over the 21<sup>st</sup> century, then the lifetimes  
of N<sub>2</sub>O and CFC-12 might drop by 20%. Thus CFCs will be cleared out of the atmosphere earlier than  
currently projected. The climate impact of N<sub>2</sub>O emissions will drop because their decay time will fall  
195 from 110 yr to 90 yr. Note that the decay time of a pulse based on a lifetime of 117 yr is reduced by a  
factor of 0.94 due to chemical feedbacks (Prather, 1998; Prather et al., 2015). Overall, we will see an



accelerated removal of the long-lived trace gases. The chemistry-climate model intercomparison projects should encourage the calculation of N<sub>2</sub>O and CFC lifetimes over the 21<sup>st</sup> century as a straightforward diagnostic of changing BDC.

200

There is an additional wrinkle in this analysis. We find that the production of NO was not increasing as fast as the loss of N<sub>2</sub>O, although admittedly the uncertainties overlap. This is expected because NO production peaks lower in the stratosphere and the rapid increase in loss above 10 hPa (~32 km) produces proportional much less NO (see P2015, Figure 1). This result supports a finding in the analysis of Froidevaux et al. (2022), where the abundance of NO and NO<sub>2</sub> in the upper stratosphere is increasing at a rate much less than that of N<sub>2</sub>O (approximately 2 vs. 12 %/decade); however, the abundance of NO in the tropical upper stratosphere is a balance between production, vertical transport, and photochemical loss above 40 km, and cannot be estimated from the production alone. Since this NO production is the cause of O<sub>3</sub> depletion by N<sub>2</sub>O in the middle stratosphere, we may find that an enhanced BDC makes N<sub>2</sub>O less important as an ozone-depleting gas from both lifetime changes and NO yields.

*Data Availability.* The raw data used here were downloaded from the sites and at the dates specified. The time series calculated here and shown in the figures are included in Tables S1-S5 in the Supplement.

*Supplement.* The Supplement related to this article is available online at: <https://doi.org/10.5194/acp-22-.....>

*Author Contributions.* MJP designed the research and performed the data analysis. LF and NJL analysed the accuracy of the datasets. MJP wrote the paper. LF and NJL reviewed and edited the paper.





*Competing interests.* The contact author has declared that neither they nor their co-authors have any  
225 competing interests

*Acknowledgments.* We thank J.L. Neu for helpful framing discussions and other MLS team members  
(Alyn Lambert, William Read, and Ryan Fuller) who contributed to the MLS v4 and v5 data sets used  
here ( $\text{O}_3$ , T, and especially  $\text{N}_2\text{O}$ ).

230

*Financial support.* Research at the University of California Irvine was supported by grants from the  
National Aeronautics and Space Administration's Atmospheric Chemistry Modeling and Analysis  
Program (ACMAP; grant no. 80NSSC21K1454) and the National Science Foundation's Atmospheric  
Chemistry Program (grant no. AGS-2135749). Work at the Jet Propulsion Laboratory was performed  
235 under contract with NASA (80NM0018D0004).

## References

- Abalos, M., Calvo, N., Benito-Barca, S., Garny, H., Hardiman, S. C., Lin, P., Andrews, M. B., Butchart,  
N., Garcia, R., Orbe, C., Saint-Martin, D., Watanabe, S., and Yoshida, K.: The Brewer–Dobson  
240 circulation in CMIP6, *Atmos. Chem. Phys.*, 21, 13571–13591, <https://doi.org/10.5194/acp-21-13571-2021>, 2021.
- Bernath P. F., Steffen J., Crouse J., and Boone C. D.: Sixteen-year trends in atmospheric trace gases  
from orbit, *J. Quant. Spectrosc. Ra.* 253, 107178, <https://doi.org/10.1016/j.jqsrt.2020.107178>, 2020.
- Butchart, N. (2014), The Brewer-Dobson circulation, *Rev. Geophys.*, 52, 157–184,  
245 doi:10.1002/2013RG000448.
- Dlugokencky, E. (2022) Data from the NOAA web site, [www.esrl.noaa.gov/gmd/ccgg/trends\\_n2o/n2o\\_mm\\_gl.txt](http://www.esrl.noaa.gov/gmd/ccgg/trends_n2o/n2o_mm_gl.txt) [pulled 2022-07-26], ed.dlugokencky@noaa.gov
- Fritsch, F., Garny, H., Engel, A., Bönisch, H., and Eichinger, R.: Sensitivity of age of air trends to the  
derivation method for non-linear increasing inert  $\text{SF}_6$ , *Atmos. Chem. Phys.*, 20, 8709–8725,  
250 <https://doi.org/10.5194/acp-20-8709-2020>, 2020.
- Froidevaux, L., Kinnison, D. E., Wang, R., Anderson, J., and Fuller, R. A.: Evaluation of CESM1  
(WACCM) free-running and specified dynamics atmospheric composition simulations using global  
multispecies satellite data records, *Atmos. Chem. Phys.*, 19, 4783–4821,  
<https://doi.org/10.5194/acp-19-4783-2019>, 2019.
- 255 Froidevaux, L., Kinnison, D. E., Santee, M. L., Millán, L. F., Livesey, N. J., Read, W. G., Bardeen, C.  
G., Orlando, J. J., and Fuller, R. A.: Upper stratospheric  $\text{ClO}$  and  $\text{HOCl}$  trends (2005–2020): Aura  
Microwave Limb Sounder and model results, *Atmos. Chem. Phys.*, 22, 4779–4799,  
<https://doi.org/10.5194/acp-22-4779-2022>, 2022.



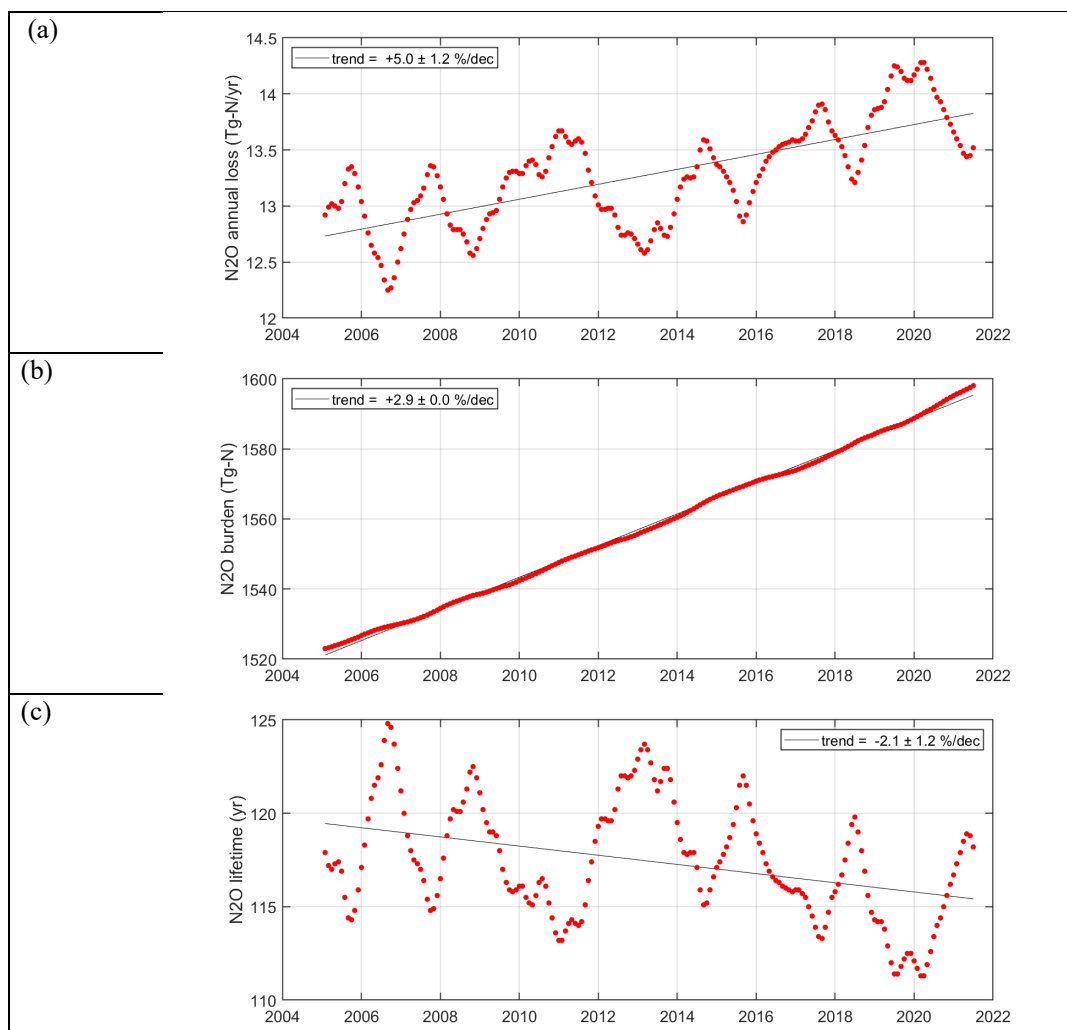
- 260 Garny, H., H. Hendon (Lead Authors), M. Abalos, G. Chiodo, A. Purich, W. Randel K. Smith and D. Thompson, Scientific Assessment of Ozone Depletion: 2022, World Meteorological Organisation Global Ozone Research and Monitoring Project-Report No. XX, WMO/UNEP Scientific Assessment of Ozone Depletion: 2022. Chapter 5: Stratospheric Ozone Changes and Climate, World Meteorological Organization, Geneva, Switzerland, 2022.
- 265 Godin-Beekmann, S., Azouz, N., Sofieva, V., Hubert, D., Petropavlovskikh, I., Effertz, P., Ancellet, G., Degenstein, D., Zawada, D., Froidevaux, L., Frith, S., Wild, J., Davis, S., Steinbrecht, W., Leblanc, T., Querel, R., Tourpali, K., Damadeo, R., Maillard-Barras, E., Stübi, R., Vigouroux, C., Arosio, C., Nedoluha, G., Boyd, I., and van Malderen, R.: Updated trends of the stratospheric ozone vertical distribution in the 60° S–60° N latitude range based on the LOTUS regression model, *Atmos. Chem. Phys. Discuss.* [preprint], <https://doi.org/10.5194/acp-2022-137>, accepted, 2022.
- 270 Karpechko, A., A. Maycock (Lead Authors), M. Abalos, J. Arblaster, H. Akiyoshi, C. Garfinkel, K. Rosenlof and M. Sigmond, Scientific Assessment of Ozone Depletion: 2018, World Meteorological Organisation Global Ozone Research and Monitoring Project-Report No. 58, WMO/UNEP Scientific Assessment of Ozone Depletion: 2018. Chapter 5: Stratospheric Ozone Changes and Climate, World Meteorological Organization, Geneva, Switzerland, 2018.
- 275 Lambert, A., Livesey, N., Read, W., and Fuller, R., MLS/Aura Level 3 Monthly Binned Nitrous Oxide (N<sub>2</sub>O) Mixing Ratio on Assorted Grids V005, Greenbelt, MD, USA, Goddard Earth Sciences Data and Information Services Center (GES DISC), Accessed: [2022-05-06], [10.5067/Aura/MLS/DATA/3545](https://doi.org/10.5067/Aura/MLS/DATA/3545), 2021.
- 280 Livesey, N. J., Read, W. G., Froidevaux, L., Lambert, A., Santee, M. L., Schwartz, M. J., Millán, L. F., Jarnot, R. F., Wagner, P. A., Hurst, D. F., Walker, K. A., Sheese, P. E., and Nedoluha, G. E.: Investigation and amelioration of long-term instrumental drifts in water vapor and nitrous oxide measurements from the Aura Microwave Limb Sounder (MLS) and their implications for studies of variability and trends, *Atmos. Chem. Phys.*, 21, 15409–15430, <https://doi.org/10.5194/acp-21-15409-2021>, 2021.
- 285 Neu, J. L., and Plumb, R. A., Age of air in a “leaky pipe” model of stratospheric transport, *J. Geophys. Res.*, 104( D16), 19243– 19255, doi:10.1029/1999JD900251, 1999.
- Plumb, R. A., and J. D. Mahlman, The zonally-averaged transport characteristics of the GFDL general circulation/tracer model, *J. Atmos. Sci.*, 44, 298–327, doi: 10.1175/1520-0469(1987)044%3C0298:TZATCO%3E2.0.CO;2, 1987.
- 290 Prather, M.J., Time scales in atmospheric chemistry: coupled perturbations to N<sub>2</sub>O, NO<sub>y</sub>, and O<sub>3</sub>, *Science*, 279, 1339-1341, 1998.
- Prather, M.J., C.D. Holmes, and J. Hsu, Reactive greenhouse gas scenarios: Systematic exploration of uncertainties and the role of atmospheric chemistry, *Geophys. Res. Lett.*, 39, L09803, 5 pp., doi:10.1029/2012GL051440, 2012.
- 295 Prather, M.J., J. Hsu, N.M. DeLuca, C.H. Jackman, L.D. Oman, A.R. Douglass, E.L. Fleming, S.E. Strahan, and S.D. Steenrod, O.A. Søvde, I.S.A. Isaksen, L. Froidevaux, and B. Funke Measuring and modeling the lifetime of nitrous oxide including its variability, *J. Geophys. Res. Atmos.*, 120, 5693–5705. doi: 10.1002/2015JD023267, 2015.
- 300 Ruiz, Daniel J., Michael J. Prather, Susan E. Strahan, Rona L. Thompson, Lucien Froidevaux, Stephen D. Steenrod, How atmospheric chemistry and transport drive surface variability of N<sub>2</sub>O and CFC-



11. J. Geophys. Res.: Atmospheres, 126, e2020JD033979. <https://doi.org/10.1029/2020JD033979>, 2021.

305 Schwartz, M., Livesey, N., Read, W., and Fuller, R., MLS/Aura Level 3 Monthly Binned Temperature on Assorted Grids V005, Greenbelt, MD, USA, Goddard Earth Sciences Data and Information Services Center (GES DISC), Accessed: [2022-07-26] [Data Access Date], 10.5067/Aura/MLS/DATA/3550, 2021a.

310 Schwartz, M., Froidevaux, L., Livesey, N., Read, W., and Fuller, R., MLS/Aura Level 3 Monthly Binned Ozone (O3) Mixing Ratio on Assorted Grids V005, Greenbelt, MD, USA, Goddard Earth Sciences Data and Information Services Center (GES DISC), Accessed: [2022-05-06, yrs 2004 & 2021 re-pulled on 2022-07-06], 10.5067/Aura/MLS/DATA/3546, 2021b.



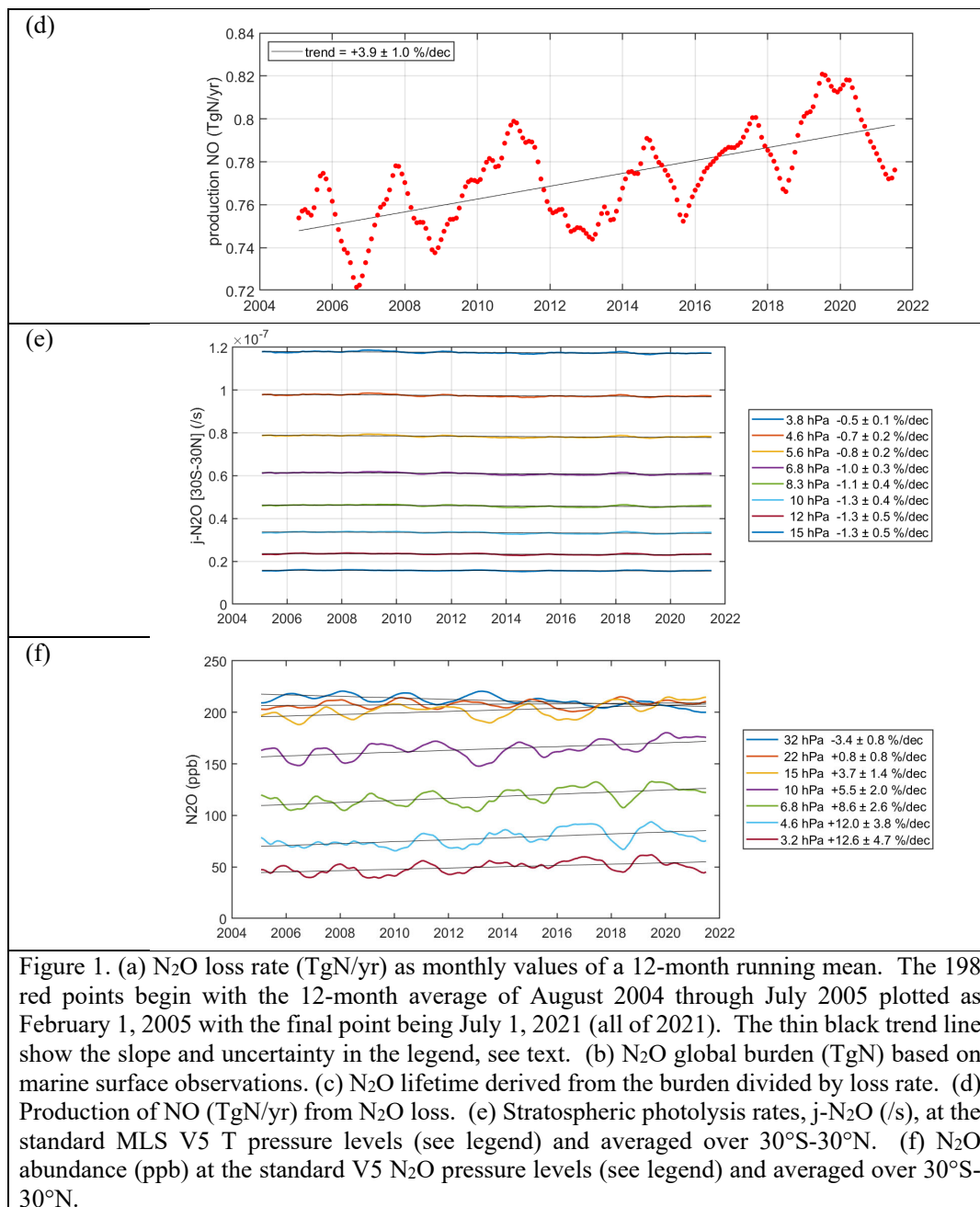


Figure 1. (a) N<sub>2</sub>O loss rate (TgN/yr) as monthly values of a 12-month running mean. The 198 red points begin with the 12-month average of August 2004 through July 2005 plotted as February 1, 2005 with the final point being July 1, 2021 (all of 2021). The thin black trend line show the slope and uncertainty in the legend, see text. (b) N<sub>2</sub>O global burden (TgN) based on marine surface observations. (c) N<sub>2</sub>O lifetime derived from the burden divided by loss rate. (d) Production of NO (TgN/yr) from N<sub>2</sub>O loss. (e) Stratospheric photolysis rates,  $j\text{-N}_2\text{O}$  (/s), at the standard MLS V5 T pressure levels (see legend) and averaged over 30°S-30°N. (f) N<sub>2</sub>O abundance (ppb) at the standard V5 N<sub>2</sub>O pressure levels (see legend) and averaged over 30°S-30°N.